2016-12-12

Bearing-only formation control with auxiliary distance measurements, leaders, and collision avoidance

Tron, Roberto

Bearing-only formation control with auxiliary distance measurements, leaders, and collision avoidance

Roberto Tron, Justin Thomas, Giuseppe Loianno, Kostas Daniilidis, and Vijay Kumar

***Abstract*— We address the controller synthesis problem for distributed formation control. Our solution requires only relative bearing measurements (as opposed to full translations), and is based on the exact gradient of a Lyapunov function with only *global* minimizers (independently from the formation topology). These properties allow a simple proof of global asymptotic convergence, and extensions for including distance measurements, leaders and collision avoidance. We validate our approach through simulations and comparison with other state-of-the-art algorithms.**

I. Introduction

The goal of formation control is to move a group of agents in order to achieve and maintain a set of desired relative positions. This task has applications in many fields such as surveillance, exploration, and transportation [2], [16], [19], [25], [29], [35]. Formations also allow the control of a large number of agents by a single human operator, and provide robustness to the failure of single agents.

The formation control problem dates back to early work on multi-robot control [4], [12]. Since then, there has been extensive work considering different control strategies (e.g., with [13], [17] or without leader nodes [2]), inter-agent sensing methodologies (positions [7], [22], distances [2], or, as reviewed below, relative directions), types of sensing or constraint graph (e.g., with limits on the number of agents [2], [8], or on the graph topology [14], [37]), strategies for connectivity control [36], models for the agents (simple integrators, non-holonomic [13], [17], second order integrators [30]), and collision avoidance mechanisms [10], [20].

In the last decade, there has been an increasing interest in vision-based solutions, where each agent is equipped with an onboard camera (early examples are [11], [21], [28]). In this setting, relative direction measurements (i.e., *bearing measurements*) are often more reliable than the corresponding distance measurements. Therefore, there has been a recent emphasis on minimizing the use of distance measurements.

Review of prior work. Given the extent of the literature, we focus only on works based on bearing-based formations. With a goal similar to ours, [7], [9] and [6] propose a distributed control law for pure bearing or mixed bearing and distance formations. However, in order to be implemented, the law also requires the distance measurements corresponding to each bearing measurement. The control strategy proposed by [14] requires only one or no distance measurements, and the control law, under ideal conditions, produces linear trajectories. In turn, however, they rely on special graph structures (where all agents can communicate and measure their relative bearings with respect to two leader agents) or on the use of distributed estimators (which "virtually" realize the unavailable measurements but are not formally considered in the stability analysis). The paper most similar to our work is [38], which proposes a bearing-only control law based on projection operators. The control law is based on a modified gradient where the (unknown) distances are removed. The stability analysis, however, does not use this fact, and crucially relies on the state of the entire network evolving on a sphere.

In most of the work above, it is assumed that the agents share or can agree on a common rotational frame (i.e., a common sense of "direction"). This can be fullfilled with a rotation localization algorithm [26], [28], [34]. The paper [38] is the only one to include a formal analysis of the effects of such localization algorithms on bearing-only formation control. On the other hand, [8] and [37] do not require a common rotational frame, but their approaches are limited to, respectively, triangular and 2-D formations with graphs containing a single cycle.

Regarding collision avoidance, this topic also has a long history [3]. Optimal solutions have been proposed [31], but they do not scale well to multiple agents and distributed settings. A more common approach is to employ local mechanisms based on either a modified potential function [18], [24], compositions of vector fields [15], [23], or constraints on the computed control laws [5], [10], [20]. All these methods, however, assume full relative state information between obstacles and agents, and are hence incompatible with bearing-only formulations.

Paper contributions. We present a formation control solution that can work with bearing measurements alone, or can be augmented with corresponding distances. As in the majority of the literature, we assume that (a) each agent can be modeled as a single integrator; (b) each agent is equipped with omnidirectional sensors (no field of view constraints); (c) the agents can agree on a common rotational frame. With respect to existing work (and in particular [14], [38]), our key contribution is to propose a control law based on the exact gradient of a Lyapunov function with global convergence guarantees (Theorem 1). While unknown distances and the full formation graph appear in the cost, the resulting control

Roberto Tron is with the Mechanical Engineering Department at Boston University, Boston 02215. The other authors are with the GRASP Lab, University of Pennsylvania, Philadelphia, Pennsylvania 19104

The authors gratefully acknoledge support from ARL grant W911NF-08-2-0004, ARO grant W911NF-13-1-0350, ONR grants N00014-07-1-0829, N00014-14-1-0510, N00014-15-1-2115, NSF grant IIS-1426840, CNS-1521617 and United Technologies.

Email: tron@bu.edu, {jut, loiannog, kostas, kumar}@seas.upenn.edu. An extended abstract of this work appeared (with partial results and without proofs) in [33].

does not require distance measurements, special assumptions on the formation or the use of additional estimators. We allow any number of agents, any graph topology, and any ambient dimension (2-D or 3-D). In particular, we do not require any notion of formation rigidity for the stability proof (although rigidity is necessary for convergence to the desired solution). The advantage of our gradient-based formulation is that it can be easily extended to include distance measurements (even a single one), leaders (agents that are externally controlled), and a distance-free collision avoidance mechanism that is compatible with bearing-only measurements.

II. Preliminaries

A. General notation

We use n to denote the dimensionality of the workspace (in practice, $n = 2$ or $n = 3$). We use $I_n \in \mathbb{R}^{n\times n}$ to denote the identity matrix, and $1_n, 0_n \in \mathbb{R}^n$ to denote the vector of all ones and zeros. The operator $\mathrm{stack}(v_1, \dots, v_m) = \mathrm{stack}(\{v_i\}_{i=1}^m)$ returns the vector obtained by vertically stacking its arguments. The angle between two vectors is denoted as $\angle(\cdot,\cdot)$. Bold letters (e.g., $\mathbf{x}$) indicates aggregated quantities which refer to multiple agents or edges (e.g., $\mathbf{x} = \mathrm{stack}(\{x_i\}_{i\in V})$). We use $|S|$ to denote the cardinality of a set S. In general, all the quantities discussed (positions, bearing vectors, etc.) and their analysis are given with respect to a global inertial reference frame $\mathfrak{R}$. However, we will occasionally refer also to the same quantities in local reference frames $\{\mathfrak{R}_i\}_{i\in V}$ specific to each one of the agents.

We use the notation $\tilde{\cdot}$ to indicate a function evaluated along a radial line $\tilde{x}(t) = x_0 + tv$ (with specified values for x_0 and v). For instance, given a function $\varphi : \mathbb{R}^n \to \mathbb{R}$, we have $\tilde{\varphi}(t) = \varphi\big(\tilde{x}(t)\big)$. With this notation, the gradient of φ at x_0 can be defined as the vector $\mathrm{grad}\,\varphi \in \mathbb{R}^n$ such that

$$\mathrm{grad}\,\varphi(x_0)^{\mathrm{T}} v = \frac{\mathrm{d}}{\mathrm{d}t}\tilde{\varphi}\bigg|_{t=0} \tag{1}$$

for any choice of v for $\tilde{x}$ (note that the value of (1) can also be interpreted as the Lie derivative of φ along v). The definition of gradient in (1) is equivalent to the one as a vector of derivatives.

B. Formations and measurements

In this subsection, we give a formal definition of a formation and of the available measurements. We identify the set of N agents as $V = \{1, \dots, N\}$, and their location as $\{x_i\}_{i\in V}$, $x_i \in \mathbb{R}^n$. Unless otherwise noted, we assume that the agents are at distinct locations, $x_i \neq x_j$ for all $i, j \in V$. We define the *range* (or *distance*) between nodes $i, j \in V$ as

$$d_{ij}(x_i, x_j) = \|x_j - x_i\|, \tag{2}$$

and the *bearing direction* (or simply *bearing*) as

$$\beta_{ij}(x_i, x_j) = d_{ij}^{-1}(x_j - x_i). \tag{3}$$

We define a *bearing+distance formation* $(\mathcal{F}, \mathbf{x})$ where:

- $\mathbf{x} = \mathrm{stack}(\{x_i\}_{i\in V})$ is the *configuration* of the formation and specifies the position of each agent in $\mathbb{R}^n$.
- $\mathcal{F} = (V, E_b, E_d)$ is a double graph in which $E_b \subseteq V \times V$ (resp., $E_d \subset E_b$) contains the set of pairs (i, j) for which agent i can measure the bearing β_{ij} (resp., the range d_{ij}). We assume that E_b and E_d are symmetric, i.e., if $(i, j) \in E_b$, then also $(j, i) \in E_b$ (the same for E_d).

We stress the assumption $E_d \subseteq E_b$, i.e., that agent i can measure the distance d_{ij} only if it can also measure the bearing β_{ij}. Our gradient-based approach could be extended to *mixed formations* with general E_d, but our results cannot guarantee global convergence in this case. For the particular case when $E_d = \emptyset$, we call $\mathcal{F}$ a *pure bearing formation*. We simply use *formation* when the distinction is not necessary. We assume that the formation $\mathcal{F}$ is fixed. In general, we use the subscript ij to indicate a scalar index corresponding to edge (i, j) in any arbitrary ordering of the edges.

For convenience, we collect the different sets of measurements in aggregate vectors as

$$\boldsymbol{\beta}(\mathbf{x}) = \mathrm{stack}(\{\beta_{ij}\}_{(i,j)\in E_b}), \tag{4}$$

$$\mathbf{d}(\mathbf{x}) = \mathrm{stack}(\{d_{ij}\}_{(i,j)\in E_d}). \tag{5}$$

Given measurements $\boldsymbol{\beta}_g \in \mathbb{R}^{n|E_b|}$, $\mathbf{d}_g \in \mathbb{R}^{|E_d|}$ specifying a desired formation, we say that these are *consistent* if there exist $\mathbf{x}_g$ such that $\boldsymbol{\beta}(\mathbf{x}_g) = \boldsymbol{\beta}_g$ and $\mathbf{d}(\mathbf{x}_g) = \mathbf{d}_g$. We also say that $\mathbf{x}_g$ is consistent with $\boldsymbol{\beta}_g, \mathbf{d}_g$.

We call a formation *leaderless* if every agent follows the same control strategy and does not require external information. We say that a formation is *leader-based* if one or more agents follows an independently specified trajectory.

For the collision avoidance extension in Section VI, we denote r as the radius of a sphere around each agent that represents its "collision zone". More precisely, agents i and j are in collision if $d_{ij} < r$. We assume that each agent does not know r, but instead can measure, for each agent j that needs to avoid, the cone $\mathcal{S}_{ij}$ with vertex at x_i and supporting the set $\{x \in \mathbb{R}^n : d(x, x_j) < r\}$ (see Figure 1a for an illustration).

C. Equivalence and rigidity of formations

Two formations $(\mathcal{F}, \mathbf{x})$ and $(\mathcal{F}, \mathbf{x}')$ are said to be:

- *Equivalent* if they produce the same measurements; that is, $\beta_{ij}(x_{g,i}, x_{g,j}) = \beta_{g,ij}$ for all $(i, j) \in E_b$ and $d_{ij}(x_{g,i}, x_{g,j}) = d_{g,ij}$ for all $(i, j) \in E_d$.
- *Identical* if they have the same configuration, $\mathbf{x} = \mathbf{x}'$.
- *Congruent* if they have the same shape and scale, that is, $\mathbf{x}'$ and $\mathbf{x}$ are related by a translation $t \in \mathbb{R}^n$ (i.e., $x'_i = x_i + t$).
- *Similar* if they have the same shape, that is, $\mathbf{x}'$ and $\mathbf{x}$ are related by a translation t and dilation $\alpha > 0$ ($x'_i = \alpha x_i + t$).

Note that similar and congruent configurations are always equivalent, but the converse might not be true. We then say that a formation is *rigid* if all formations equivalent to it are also similar (for the case of pure bearing formations) or congruent (for the case of bearing+distance formations).

In practice, one can check whether a formation is rigid by checking the rank of the so called *rigidity matrix* (see [7], [27], [38] for details).

III. Formation control

In this section, we formulate the problem of formation control for a network of kinematic agents and propose our gradient-based solution. For the moment, we consider only leaderless formations (that is, all agents follow the same strategy). Leader-based formations are considered in Section VI. The main feature of our method is the global asymptotic convergence of the closed loop system to a configuration equivalent to the desired $\mathbf{x}_g$. Rigidity, although not specifically required in the proofs, will then imply rigid equivalence.

We assume that each agent $i \in V$ follows the model $\dot{x}_i(t) = u_i$, where u_i is a control input. In vector notation, we have $\dot{\mathbf{x}}(t) = \mathbf{u}$ where $\mathbf{u} = \mathrm{stack}\big(\{u_i\}_{i\in V}\big)$. Given desired measurements $\boldsymbol{\beta}_g, \mathbf{d}_g$ which are consistent with a desired rigid formation $(\mathcal{F}, \mathbf{x}_g)$, our goal is to design inputs $\mathbf{u}$ that drive the agents into a configuration equivalent to $\mathbf{x}_g$. Our control law is the negative gradient of a cost function $\varphi(\mathbf{x})$, $\mathbf{u} = -\operatorname{grad}\varphi(\mathbf{x})$. By carefully defining the structure of φ, this law can be directly computed from the available measurements (as mentioned before, this is in contrast to previous work where additional information such as distance measurements is generally required).

A. The cost function

The cost function we propose is of the following form:

$$\varphi(\mathbf{x}) = \alpha_b \sum_{(i,j)\in E_b} \varphi^b_{ij}(x_i, x_j) + \alpha_d \sum_{(i,j)\in E_d} \varphi^d_{ij}(x_i, x_j), \quad (6)$$

$$\varphi^b_{ij}(x_i, x_j) = d_{ij} f_b\big(c_{ij}\big), \quad (7)$$

$$\varphi^d_{ij}(x_i, x_j) = f_d\big(q_{ij}\big). \quad (8)$$

We now proceed to explain the various parts of this equation (the reader is invited to refer back to (6) as we proceed). At a high level, φ is composed of a summation, weighted by $\alpha_b, \alpha_d > 0$, over the edges E_b and E_d. Each term in the summation is a function of one of the two following "similarity measures" between the current measurements $\boldsymbol{\beta}(\mathbf{x}), \mathbf{d}(\mathbf{x})$ and the desired ones, $\boldsymbol{\beta}_g, \mathbf{d}_g$:

$$c_{ij}(x_i, x_j) = \beta^{\mathrm{T}}_{g,ij}\beta_{ij} = \cos\big(\angle(\beta_{g,ij}, \beta_{ij})\big), \quad (i,j) \in E_b \quad (9)$$

$$\begin{aligned} q_{ij}(x_i, x_j) &= \beta^{\mathrm{T}}_{g,ij}\big(x_j - x_i - (x_{g,j} - x_{g,i})\big) \\ &= \beta^{\mathrm{T}}_{g,ij}(d_{ij}\beta_{ij} - d_{g,ij}\beta_{g,ij}) \\ &= d_{ij}c_{ij} - d_{g,ij}, \quad (i,j) \in E_d. \end{aligned} \quad (10)$$

Eq. (9) is the cosine of the angle between the measured and desired bearings ($c_{ij} = 1$ when the bearings coincide), while (10) quantifies the discrepancy between the measured and desired relative position of the agents projected on the line given by $\beta_{g,ij}$ ($q_{ij} = 0$ when bearing and distances coincide, see Figure 1 for an illustration). We use q_{ij} instead of a simple difference of the distances because q_{ij} is actually linear in the configuration $\mathbf{x}$ (see first line of (10)). Each of these similarities is weighted by a reshaping function f_b (for the c_{ij}'s) or f_d (for the q_{ij}'s). In this paper, we use $f_b(c) = 1 - c$ and $f_d(q) = \frac{1}{2}q^2$, but the choice of other $\mathcal{C}^2$ (i.e., twice differentiable) functions is also possible, as explained in Section V.

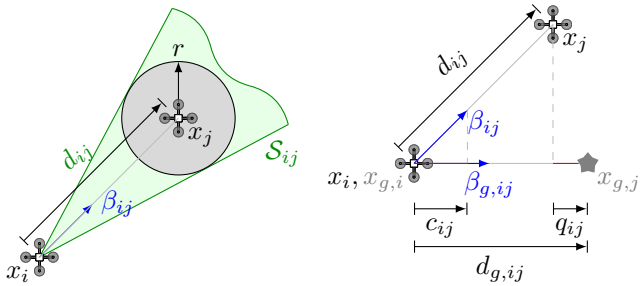

(a) (b)

Fig. 1: (a) Measurements of agent i with respect to agent j: bearing β_{ij}, distance d_{ij} and cone $\mathcal{S}_{ij}$ for collision avoidance with radius r. (b) The similarity measures c_{ij} (9), q_{ij} (10) used in φ, and defined with respect to the desired measurements $\beta_{g,ij}$, $d_{g,ij}$. ⬟: desired position for agent j, $x_{g,j}$, with respect to agent i, $x_{g,i}$.

B. The gradient and control law

Using the chain rule, the gradient of each term (7) and (8) can be computed as (see [32] for detailed derivations):

$$\begin{aligned} g^b_{ij} &= \operatorname{grad}_{x_i}\varphi^b_{ij}(x_i, x_j) \\ &= -f_b(c_{ij})\beta_{ij} - f'_b(c_{ij})(I_n - \beta_{ij}\beta^{\mathrm{T}}_{ij})\beta_{g,ij}, \end{aligned} \quad (11)$$

$$g^d_{ij} = \operatorname{grad}_{x_i}\varphi^d_{ij}(x_i, x_j) = -f'_d(d_{ij}c_{ij} - d_{g,ij})\beta_{g,ij}. \quad (12)$$

The gradient of (6) with respect to the i-th agent is then:

$$g_i = \operatorname{grad}_{x_i}\varphi(\mathbf{x}) = \alpha_b \sum_{j:(i,j)\in E_b} g^b_{ij} + \alpha_d \sum_{j:(i,j)\in E_d} g^d_{ij}. \quad (13)$$

Note that, while the cost function depends on the range d_{ij}, the gradient information for φ^b_{ij} depends only on local bearing information and no range information is necessary (this is because d_{ij} in (7) cancels out when taking the gradient).

IV. Properties of the control law

Before giving a detailed analysis of the convergence of the algorithm, we elaborate on a few of its properties.

Choice of local reference frame. The proposed control law can be computed in any local reference frame, in the sense that if β_{ij} and $\beta_{g,ij}$ are provided in either the local frame $\mathfrak{R}_i$ or the global frame $\mathfrak{R}$, then g_i will represent the control action in that same frame. Practically, this means that we can avoid unnecessary coordinate transformations during the implementation on a real platform.

This property is a direct consequence of the following proposition, which shows that the measurements, the similarity measures, and the terms for the cost function behave "as one would expect" under coordinate transformations.

Proposition 1: Let $g_{ij} = (R_{ij}, t_{ij})$ represent a common rigid transformation acting on x_i, x_j and their counterparts $x_{g,i}, x_{g,j}$. Then, the bearing vectors $\beta_{ij}(x_i, x_j)$ are invariant to the action of t_{ij}, follow the common rotation R_{ij}, and are skew-symmetric with respect to a permutation of the indexes

i and j:

$$\beta_{ij}(R_{ij}x_i + t_{ij}, R_{ij}x_j + t_{ij}) = R_{ij}\beta_{ij}(x_i, x_j) \quad (14)$$
$$\beta_{ij}(x_i, x_j) = -\beta_{ji}(x_j, x_i). \quad (15)$$

Additionally, the quantities d_{ij}, c_{ij}, q_{ij}, φ^b_{ij} and φ^d_{ij} are all invariant to R_{ij}, t_{ij} and permutation of the indexes:

$$d_{ij}(R_{ij}x_i + t_{ij}, R_{ij}x_j + t_{ij}) = d_{ij}(x_i, x_j) \quad (16)$$
$$d_{ij}(x_i, x_j) = d_{ji}(x_j, x_i), \quad (17)$$

with similar expressions for the other quantities.

Proof: Eqs. (14)–(17) directly follow from the definitions of d_{ij} and β_{ij}. These can then be used to prove the invariance properties for c_{ij}, q_{ij}. Since φ^b_{ij} and φ^d_{ij} are functions of c_{ij} and q_{ij}, their properties follow as well. ∎

We used the notation g_{ij} to underline the fact that, in principle, we can have different a different rotation and translation pair for each edge. This is needed in the convergence proof of Section V. Nevertheless, we stress the fact that these *do not* represent physical transformations, but only convenient analytical tools.

Correspondence-less control. For $f_b(c) = 1 - c$ and pure bearing formations, we have $f'_b(c) = -1$. Recalling that $c_{ij} = \beta^{\mathrm{T}}_{ij}\beta_{g,ij}$, the gradient (11) becomes: $g^b_{ij} = \beta_{g,ij} - \beta_{ij}$. Then, our control law simplifies to:

$$u_i = \alpha_b \sum_{j:(i,j)\in E} \beta_{g,ij} - \alpha_b \sum_{j:(i,j)\in E} \beta_{ij}, \quad (18)$$

which contains two (unordered) sums. Each sum can be computed independently without explicitly associating each $\beta_{g,ij}$ with its corresponding β_{ij} (in fact, the first sum could be precomputed offline). As a result, we say that the law is *correspondence-less*.

Centroid invariance. Since the gradient follows the structure of a symmetric network, we have the following:

Proposition 2: The centroid $\bar{x} = \frac{1}{|V|}\sum_{i\in V} x_i$ is invariant with respect to the trajectories of the closed loop system (i.e., $\dot{\bar{x}} = 0$).

Proof: Proposition 1 applied in (11) and (12) implies the following anti-symmetry of the gradients: $g^b_{ij} = -g^b_{ji}$, $g^d_{ij} = -g^d_{ji}$. The evolution of $\bar{x}$ is given by

$$\begin{aligned}\dot{\bar{x}} &= \frac{1}{N}\sum_{i\in V}\Big(\alpha_b \sum_{j:(i,j)\in E_b} g^b_{ij} + \alpha_d \sum_{j:(i,j)\in E_d} g^d_{ij}\Big) \\ &= \frac{\alpha_b}{N}\sum_{(i,j)\in E_b}(g^b_{ij} + g^b_{ji}) + \frac{\alpha_d}{N}\sum_{(i,j)\in E_d}(g^d_{ij} + g^d_{ji}) = 0,\end{aligned} \quad (19)$$

that is, the centroid is invariant under the trajectories of our proposed controller. ∎

Proposition 2 has two practical implications. First, the final centroid of the configuration will be identical to the initial one (i.e., the average of the positions of the agents remains constant without any drift). Second, since the relation between the centroid and the configuration is linear, we could leverage the superposition principle to control the position of the centroid of the formation by adding the exogenous control of a "virtual leader" to one of the agents.

V. Stability analysis

In this section, we prove convergence of our control law to the desired formation from any initial condition. We split the analysis into two steps. In the first step, we show that the set of global minimizers of φ corresponds exactly with the set of configurations $\mathbf{x}$ equivalent to $\mathbf{x}_g$. We also show that these are the only critical points of φ (i.e., points where $\operatorname{grad}\varphi(\mathbf{x}) = 0$). In the second step, we add technical results showing that the trajectories of the closed-loop system do not diverge, thus showing global asymptotic stability.

For our analysis, we will leverage some of the ideas from [32], but with significant extensions due to the fact that here we consider a multi-agent problem, while [32] focuses on a single-agent problem (visual homing).

A. Global minimizers and critical points

In order for the results in this section to hold, the functions f_b and f_d introduced in Section III-A must adhere to the following definitions.

Definition 1: The function $f_b : [-1, 1] \to \mathbb{R}$ is $\mathcal{C}^2$ and:

$$f_b(c) \geq 0, \text{ with equality iff } c = 1, \quad (20)$$
$$f'_b(c) \text{ is finite} \quad (21)$$
$$f'_b(c) \begin{cases} \leq 0 & \text{for } c = 1, \\ < 0 & \text{otherwise,} \end{cases} \quad (22)$$
$$f_b(c) + (1 - c)f'_b(c) \leq 0. \quad (23)$$

Definition 2: The function $f_d : \mathbb{R} \to \mathbb{R}$ is $\mathcal{C}^2$ and:

$$f_d(q) \geq 0, \text{ with equality iff } q = 0, \quad (24)$$
$$\operatorname{sign}(f'_d(q)) = \operatorname{sign}(q), \quad (25)$$
$$f''_d(0) > 0. \quad (26)$$

Properties (20), (22), (24)–(26) are general statements to ensure that these functions can be used as similarity measures (i.e., lower values correspond to measurements closer to the desired ones) and that f_d is locally quadratic near the origin. Eq. (23) is a technical property which required later.

With these definitions, we can state our first result on the global minimizers of the cost function. The proof is based on the non-negativity of each term in φ.

Lemma 1: A configuration $\mathbf{x}$ is a global minimizer of φ if and only if it is equivalent to $\mathbf{x}_g$.

Proof: From the fact that $d_{ij} > 0$ and from the properties of f_b (respectively, f_d), each term φ^b_{ij} (resp., φ^d_{ij}) is non-negative, and it is zero if and only if $c_{ij} = 1$ and $\beta_{ij}(x_i, x_j) = \beta_{g,ij}$ (and, respectively, $q_{ij} = 0$ and $d_{ij}(x_i, x_j) = d_{g,ij}$). By definition, $\mathbf{x}$ is then equivalent to $\mathbf{x}_g$. ∎

Now, we need to show that there are no other critical points of φ. Since φ is non-convex, we analyze the function by considering radial lines in $\mathbb{R}^{n|V|}$ starting from a global minimizer (a configuration equivalent to $\mathbf{x}_g$) and going in any arbitrary direction. By showing that the cost along these lines is always increasing, and using (1), it follows that φ does not have any other critical point. We start by considering each individual term in φ using radial lines in $\mathbb{R}^{2n}$.

Lemma 2: Define the line $\big(\tilde{x}_i(t), \tilde{x}_j(t)\big) = (x_{i0}+tv_i, x_{j0}+tv_j)$, where $v_i, v_j \in \mathbb{R}^n$ are arbitrary and where (x_{i0}, x_{j0}) are such that $\beta_{ij}(x_{i0}, x_{j0}) = \beta_{g,ij}$. Define $v = v_j - v_i$. Under the conditions in Definition 1, the derivative of the function

$$\tilde{\varphi}^b_{ij}(t) = \varphi^b_{ij}\big(\tilde{x}_i(t), \tilde{x}_j(t)\big) \tag{27}$$

satisfies the following. If $t = 0$ or $v = 0$, then $\dot{\tilde{\varphi}}^b_{ij} = 0$. Otherwise, for $v \neq 0$ and for all $t > 0$, $\dot{\tilde{\varphi}}^b_{ij} > 0$, except when:

- If $v = a\beta_{g,ij}$, $a < 0$, for which $\dot{\tilde{\varphi}}^b_{ij} \equiv 0$.
- If $v = a\beta_{g,ij}$, $a > 0$, for which

$$\dot{\tilde{\varphi}}^b_{ij} \begin{cases} \equiv 0 & \text{for } t \in \left[0, \frac{\|x_{j0}-x_{i0}\|}{\|v\|}\right), \\ > 0 & \text{for } t > \frac{\|x_{j0}-x_{i0}\|}{\|v\|}. \end{cases} \tag{28}$$

Proof: The proof extends and relies on [32, Lemma 3.6]. Define the following change of variables: $\tilde{x}'(t) = \tilde{x}_j(t) - \tilde{x}_i(t)$, $x'_g = \tilde{x}'(0)$, $x'_i = 0$, $y'_{gi} = \beta_{ij}(x'_g, x'_i)$, $\tilde{y}'_i = \beta_{ij}(\tilde{x}'_i, x_i)$. Note $\dot{\tilde{x}}'(t) = v$. From the invariance of φ_{ij} given by Proposition 1, we have

$$\varphi^b_{ij}\big(\tilde{x}_i(t), \tilde{x}_j(t)\big) = \varphi^b_{ij}\big(0, \tilde{x}_j(t) - \tilde{x}_i(t)\big) \tag{29}$$

$$= d_{ij}(x'_g, \tilde{x}) f_b({y'_{gi}}^{\mathrm{T}} \tilde{y}'_i), \tag{30}$$

which is of the same form as $\tilde{\varphi}_i$ in [32, Lemma 3.6]. The claim is then simply a restatement of that lemma with our change of variables. ∎

Lemma 3: Define the line $\big(\tilde{x}_i(t), \tilde{x}_j(t)\big) = (x_{i0}+tv_i, x_{j0}+tv_j)$, where $v_i, v_j \in \mathbb{R}^n$ are arbitrary and where (x_{i0}, x_{j0}) are such that and $x_{j0} - x_{i0} = d_{g,ij}\beta_{g,ij}$, i.e., x_{j0} and x_{i0} are consistent with both $d_{g,ij}$ and $\beta_{g,ij}$. Under the conditions on f_d of Definition 1, the derivative of the function

$$\tilde{\varphi}_{ij}(t) = \varphi^d_{ij}\big(\tilde{x}_i(t), \tilde{x}_j(t)\big) \tag{31}$$

has the property

$$\dot{\tilde{\varphi}}_{ij}(t) \begin{cases} \geq 0, \text{ with equality iff } t = 0, \text{ when } v^{\mathrm{T}}\beta_{g,ij} \neq 0 \\ \equiv 0, \text{ when } v^{\mathrm{T}}\beta_{g,ij} = 0. \end{cases} \tag{32}$$

Proof: Define $v = v_j - v_i$ and note that (8) can be rewritten as

$$\tilde{\varphi}_{ij} = \varphi^d_{ij}(\tilde{x}_i, \tilde{x}_j) = f_d\Big(\beta^{\mathrm{T}}_{g,ij}\big(\tilde{x}_i - \tilde{x}_j - (x_{g,i} - x_{g,j})\big)\Big)$$
$$= f_d\Big(\beta^{\mathrm{T}}_{g,ij}\big(d_{g,ij}\beta_{g,ij} + tv - d_{g,ij}\beta_{g,ij}\big)\Big) = f_d(t\beta^{\mathrm{T}}_{g,ij}v). \tag{33}$$

Taking the derivative, we have

$$\dot{\tilde{\varphi}}_{ij} = f'_d(t\beta^{\mathrm{T}}_{g,ij}v)\beta^{\mathrm{T}}_{g,ij}v. \tag{34}$$

The claim then follows from the properties of f_d. ∎

We can now combine these two lemmata and give the main result of this section.

Proposition 3: The function φ has global minimizers at configurations equivalent to $\mathbf{x}$ which are consistent with $\mathcal{F}$ and no other critical points.

Proof: As before, let $\mathbf{x}_g$ be a configuration consistent with $\mathcal{F}$. Consider any arbitrary configuration $\mathbf{x}_0 \neq \mathbf{x}_g$ and define $\tilde{\mathbf{x}}(t) = \mathbf{x}_g + t(\mathbf{x}_0 - \mathbf{x}_g)$. Notice that $\tilde{\mathbf{x}}(0) = \mathbf{x}_g$ and $\tilde{\mathbf{x}}(1) = \mathbf{x}_0$. By linearity, we have

$$\frac{\mathrm{d}}{\mathrm{d}t}\varphi(\tilde{\mathbf{x}})\Big|_{t=1} = \sum_{(i,j)\in E_b} \frac{\mathrm{d}}{\mathrm{d}t}\tilde{\varphi}^b_{ij}(t)\Big|_{t=1} + \sum_{(i,j)\in E_d} \frac{\mathrm{d}}{\mathrm{d}t}\tilde{\varphi}^d_{ij}(t)\Big|_{t=1}. \tag{35}$$

From Lemmata 2 and 3, each term on the RHS of (35) will be non-negative. We then have two cases.

1) All the terms on the RHS are zero (and, hence, so is the LHS). However, from the same lemmata, this implies that $\varphi(\tilde{\mathbf{x}}) \equiv 0$ at least for $t \in [0, 1]$ (and possibly for $t \in [0, \infty)$). This means that $\varphi(\tilde{\mathbf{x}}(1)) = \varphi(\mathbf{x}_0) = 0$. Therefore, $\mathbf{x}_0$ is also a global minimizer.

2) At least one of the terms on the RHS of (35) is strictly positive. In this case, $\frac{\mathrm{d}}{\mathrm{d}t}\varphi(\tilde{\mathbf{x}})\big|_{t=1} \neq 0$. Then, by the definition in (1), $\operatorname{grad}\varphi(\mathbf{x}_0) \neq 0$, and $\mathbf{x}_0$ is not a critical point. ∎

B. Convergence analysis

Our final goal is to show that the basin of attraction of the equilibria of the closed loop system is the entire space $\mathbb{R}^{Nn}$. From a technical standpoint, there is a small obstacle on the way to this goal: the gradient (13), and hence our control law, is not defined when two neighboring agents i and j have coincident positions $x_i = x_j$. This situation has scarse practical relevance, but it needs to be considered from a theoretical standpoint.

Fortunately, this difficulty can be easily sidestepped: we extend the definition of the gradient by setting to zero the terms corresponding to the edges (i, j) where $x_i = x_j$. The following lemma shows that this is equivalent to computing a sub-gradient of φ.

Lemma 4: The discontinuities of the function $\varphi^b_{ij}(x_i, x_j)$ on the subspace $x_i = x_j$ can be removed by letting $\varphi^b_{ij}(x_i, x_j) = 0$. Then, a subgradient of φ^b_{ij} at any point on the same subspace is given by $\operatorname{grad}\varphi^b_{ij}(x_i, x_j) = 0_{2n}$.

Proof: From Definition 1, one can deduce that f_b is bounded above. Since $d_{ij}(x_i, x_j) = 0$ when $x_i = x_j$, we then have that $\lim_{x_i - x_j \to 0} \varphi^b_{ij}(x_i, x_j) = 0$, independently of the path taken by x_i and x_j. This shows that the discontinuities can be removed. Then, since $d_{ij} \geq 0$ and $f_b(c) \geq 0$, also $\varphi^b_{ij}(x_i, x_j) \geq 0$. This means that $f(x'_i, x'_j) - f(x_i, x_j) \geq 0$ for any $x'_i, x'_j \in \mathbb{R}^n$ and $x_i = x_j$. Hence, by definition, 0_{2n} is a subgradient of φ^b_{ij} at $x_i = x_j$. ∎

We are now ready to show our main convergence result:

Theorem 1: Any trajectory of the closed-loop system

$$\dot{\mathbf{x}} = -\operatorname{grad}\varphi(\mathbf{x}) \tag{36}$$

asymptotically converges to a configuration which is equivalent to the desired one $\mathbf{x}_g$.

Since our closed-loop is a gradient system, standard arguments give us convergence to the set of critical points of φ. However, there are a couple of technical aspects which we need to consider, mostly due to the fact that, for leaderless pure bearing formations, the level sets of φ are not compact. First, we need to show that the trajectories do not diverge. Then, we need to show their convergence to a single point (as opposed to infinitely wandering in a set). Since the proof is rather

technical, the details can be skipped on a first reading without loss of continuity.

Proof: Step 1: For bearing+distance formations, we apply a change of variables in $\mathbb{R}^{Nn}$ such that $\mathbf{x}_g = 0$. For pure bearing formations, we set $\bar{x} = 0$. *Step 2:* We show that the closed loop trajectories do not diverge to infinity, i.e., $\lim_{t\to\infty}\|\mathbf{x}(t)\| \neq \infty$. Define the line $\tilde{\mathbf{x}}(s, v) = s\mathbf{v}$, where $s \in \mathbb{R}$ and $\mathbf{v} \in \mathbb{R}^{Nn}$, $\|\mathbf{v}\| = 1$. For fixed s, $\tilde{\mathbf{x}}$ describes a sphere of radius s centered at the origin. For fixed $\mathbf{v}$, the curve $\tilde{\mathbf{x}}$ describes a radial line normal to any of these spheres. Using the same argument from the proof of Proposition 3, one has that, for any arbitrary $\mathbf{v}$,

$$\frac{\mathrm{d}}{\mathrm{d}s}\varphi\big(\tilde{\mathbf{x}}(s, v)\big) = \mathbf{v}^{\mathrm{T}} \operatorname{grad}\varphi(\tilde{\mathbf{x}}) \geq 0. \tag{37}$$

By way of contradiction, if a trajectory $\mathbf{x}(t)$ diverges to infinity, then (by definition of limit) there exists a time $T > 0$ for which the trajectory escapes the ball of radius $s = \|\mathbf{x}(T)\|$. This implies that the inner product between the normal to the ball and the trajectory direction is positive, i.e.,

$$\mathbf{v}^{\mathrm{T}}\dot{\mathbf{x}} = -\mathbf{v}^{\mathrm{T}}\mathbf{g} > 0, \tag{38}$$

where $\mathbf{v}$ is given by $\mathbf{v} = \frac{\mathbf{x}}{\|\mathbf{x}\|}$. However, (38) contradicts (37). Hence the trajectories of the closed system are compact. *Step 3:* For rigid bearing+distance formations, this and Lyapunov's theorem show that the trajectories of the system converge to the unique formation which is congruent with the desired one and has the same centroid. For non-rigid bearing+distance and pure bearing formations, compactness only implies convergence to a *set* of accumulation points. *Step 4:* From compactness of $\mathbf{x}(t)$, there exists a constant $d_{\max}$ such that $d_{ij} < d_{\max}$ for all $t > 0$ and $(i, j) \in E_b$. Since the quantities $\{c_{ij}\}$ and $\{d_{ij}\}$ are, respectively, invariant and directly proportional to scaling, one can show that:

$$\|\operatorname{grad}\varphi(\alpha\mathbf{v})\| = \|\operatorname{grad}\varphi(\mathbf{v})\|, \quad \varphi(\alpha\mathbf{v}) = \alpha\varphi(\mathbf{v}) \tag{39}$$

for any $\alpha > 0$. By taking the maximum of these quantities over $\mathbf{x} = \alpha\mathbf{v}$ restricted to $\{\mathbf{x} \in \mathbb{R}^{Nn} : d_{ij} < d_{\max}\ \forall (i, j) \in E_b\}$ (which is compact), we can always choose $c > 0$ and $\mu \in [0, 1)$ (as a function of $d_{\max}$ such that

$$\|\operatorname{grad}\varphi(\mathbf{x})\| > c|\varphi(\mathbf{x})|^{\mu} \tag{40}$$

on a compact set containing $\mathbf{x}(t)$. Eq. (40) has the form of a *Lojasiewicz gradient inequality*, which can be used in the Lojasiewicz theorem to show the convergence of the trajectory $\mathbf{x}(t)$ to a single point (see the review article [1]). ∎

As mentioned in the introduction, the result of Theorem 1 does not require the notion of rigidity. However, when the two are combined, we obtain the following:

Corollary 1: Assume that the desired formation $(\mathcal{F}, \mathbf{x}_g)$ is rigid. Then any trajectory of (36) converges to a configuration which is similar (for pure bearing formations) or congruent (for bearing+distance formations) to the desired one.

VI. Extensions

In this section we use the fact that our solution is gradient-based to include leaders and a collision avoidance mechanism.

A. Leaders

Consider one or two leader nodes (say, nodes $\hat{\imath}$ and $\hat{\jmath}$) that are kept stationary ($u_{\hat{\imath}} = u_{\hat{\jmath}} = 0$). With two leaders, we assume that their relative positions are consistent with the desired formation. Intuitively, the purpose of the first leader is to fix the translation of the final formation, and the purpose of the second one is to fix the scale (when distance measurements are not available). In the one-leader case (resp., two-leader case), we remove the variable for $\hat{\imath}$ (resp. $\hat{\imath}$ and $\hat{\jmath}$) from (6) and define φ_{leader} to be equal to φ restricted to the $d(n-1)$-dimensional (resp., $d(n-2)$) affine subspace of $\mathbb{R}^{dn}$ where $x_{\hat{\imath}}$ (resp., $x_{\hat{\imath}}, x_{\hat{\jmath}}$) is constant. One can then easily verify that, for all the nodes i that are not leaders, the gradient $\operatorname{grad}_{x_i}\varphi_{leader}$ is still given by (13). The results of Proposition 3 and Theorem 1 still hold, with the only difference that $\mathbf{x}_g$ is now restricted to have a particular value for $x_{\hat{\imath}}$ (respectively, $x_{\hat{\imath}}, x_{\hat{\jmath}}$). Thus, we still have global asymptotic convergence of the control law. The only real difference between this extension and the case of leaderless formations is that the centroid invariance established in Proposition 2 does not hold anymore because the stationary leaders partially break the symmetry between the updates of the agents. Instead, the translational ambiguity of the entire formation is fixed by the initial position of the leaders.

To move the formation, one can either apply the desired controls to the leaders and use the controller to track this time-varying reference (with a possible steady-state error) or apply feed-forward terms that, however, need to be assigned to all the agents at the same time (see [14] for details).

B. Collision avoidance

We now present a proof-of-concept collision avoidance mechanism. This mechanism is loosely inspired by [10] in the fact it uses optimization-in-the-loop, but with simple integrator models and without the need to introduce distance measurements. Consider two agents i and j as in Figure 1a. Notice that the cone $\mathcal{S}_{ij}$ can be determined without knowing d_{ij}, and that $\mathcal{S}_{ij}$ represents an overestimate of the area of radius r to avoid around agent j. Therefore, as long as agent i does not enter the cone $\mathcal{S}_{ij}$, collision will be avoided. We therefore propose to modify the control u_i derived from (13) as follows. First, find a unit vector q_i that is closest to u_i but does not belong to any of the cones $\mathcal{S}_{ij}$:

$$\max_{q_i} q_i^{\mathrm{T}} u_i, \text{ s.t. } \|q_i\| = 1, q_i \neq \cup_{j:(i,j)\in E_{ca}} \mathcal{S}_{ij}, \tag{41}$$

where E_{ca} are the set of neighbors for collision avoidance (in general situations, we would like $E_a = V \times V$, as agents that are not sensed cannot be avoided). Note that, $u_i' = u_i$ when u_i does not belong to any cone. For 2-D agents, the optimization problem (41) can be solved efficiently by sorting the cones $\{\mathcal{S}_{ij}\}_{(i,j)\in E_{ca}}$ according to their angles and checking for intersections. Second, obtain a new control u_i' by projecting u_i on q_i, that is, $u_i' = q_i q_i^{\mathrm{T}} u_i$. Note that this choice implies that the controller will be stable, because the derivative of

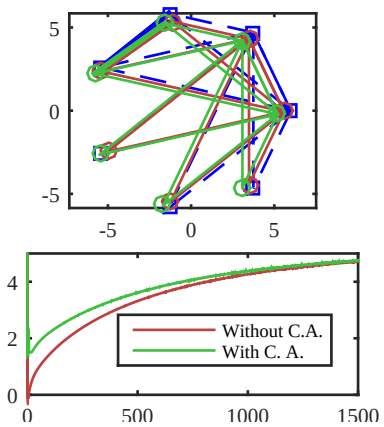

Fig. 2: Numerical example of the effect of the collision avoidance mechanism. The input u_i is given by our bearing-only controller, $E_{ca} = V \times V$ and the radius for collision avoidance is $r_i = 1.5$. The agents are initialized roughly at the opposite of the desired positions. Top: final configuration of the agents. Bottom: minimum distance between any two pair of distinct agents for the first interval of the simulation. Note that without the modified control law the agents collide toward the beginning of the simulation.

the Lyapunov function φ along the trajectories of the closed loop system will be negative semidefinite:

$$\dot{\varphi} = \sum_{i \in V} g_i^{\mathrm{T}} u_i' = -\sum_{i \in V} g_i^{\mathrm{T}} q_i q_i^{\mathrm{T}} g_i \leq 0. \tag{42}$$

In the next section we present a simulation to validate this approach, leaving a full theoretical analysis for future work.

VII. Simulations

In this section, we validate our proposed controllers through simulations using networks of seven agents in 2-D formations (results for 3-D formations are omitted due to space reasons). We compare the results with those of other controllers to show the flexibility of our approach and differences in the generated trajectories. The desired formation is set to one where all the agents are equally spaced around a circle or a sphere. The number of neighbors for each node is between 2 and 3. The initial positions of the agents are assigned at random (but remain the same throughout). We simulate four scenarios. In all cases, we compare our controller without any and with one distance measurement, and we compare with the algorith of [38]. In the first scenario we do not use leaders. For reference, the initial configuration of the agents is translated so that its centroid coincides with the centroid of the desired formation. In the second and third scenarios, we use, respectively, one and two leaders. Notice that, in these cases, the convergence proof for the method of [38] does not hold, but the control law can still be applied by ignoring the controls for the leaders. For comparison purposes, the leaders are fixed at their desired positions. In the last scenario, we use two leaders, but the graph follows the structure required by [14], so that also that method can be included in the comparison. In general, all the methods converge to the desired formations. With respect to [38], our method can converge to the correct scale by incorporating just one distance measurement for the scenarios with zero and one leaders. We can also use Theorem 1, to prove convergence with leaders (see Section VI). With respect to [14], our work and the work from [38] do not require a particular graph structure. However, the control [14] provide straight trajectories and generally faster convergence.

Finally, we include a numerical example of the behaviour of the bearing-only controller with and without collision avoidance in Figure 2. As expected, the modified controller avoids inter-agent collisions. Although for this case the agents have reached the desired configuration, we have found this not to be the case for more complicated graphs, where the agents get stuck in suboptimal positions. This is most likely due to the non-convexity of the constraints given by $\mathcal{S}_{ij}$.

VIII. Discussion and Conclusions

In this paper, we proposed a globally convergent solution for leaderless, bearing-based formation control. This gradient-based controller can be naturally complemented with additional inter-agent distance measurements and with or without the presence of leader agents. We tested our approach through simulations. The main advantage of our approach with respect to competing solutions [14], [38] is in its flexibility: we can prove global convergence for both pure bearing and bearing+distance formations with or without leaders, and include a collision avoidance mechanism, all under the same framework. This is because it is based on the exact gradient of a Lyapunov function. However, [14], [38] have their advantages in their specific domains: the control law of [38] has *exponential* convegence guarantees, and maintains the scale of the formation, while the use of triplets of agents in [14] results in very simple and fast straight trajectories. As future work, we plan to investigate strategies to incorporate these ideas in our framework.

References

[1] P.-A. Absil, R. Mahony, and B. Andrews. Convergence of the iterates of descent methods for analytic cost functions. *SIAM Journal on Optimization*, 16(2):531–547, 2005.

[2] B. D. O. Anderson, B. Fidan, C. Yu, and D. van der Walle. UAV formation Control: Theory and Application. In Springer, editor, *Recent Advance in Learning and Control*, volume 371 of *Lectures Notes in Control and Information Sciences*, pages 15–34, 2008.

[3] R. C. Arkin. *Behavior-based robotics*. MIT press, 1998.

[4] T. Balch and R. C. Arkin. Behavior-based formation control for multirobot teams. *IEEE Trans. Automat. Contr.*, 14(6):926–939, 1998.

[5] A. N. Bishop. A very relaxed control law for bearing-only triangular formation control. *IFAC Proceedings Volumes*, 44(1):5991–5998, 2011.

[6] A. N. Bishop, M. Deghat, B. D. O. Anderson, and U. Hong. Distributed formation control with relaxed motion requirements. *International Journal of Robust and Nonlinear Control*, 2014.

[7] A. N. Bishop, I. Shames, and B. Anderson. Stabilization of rigid formations with direction-only constraints. In *IEEE Int. Conf. on Decision and Control*, pages 746–752, 2011.

[8] A. N. Bishop, T. H. Summers, and B. D. O. Anderson. Control of triangle formations with a mix of angle and distance constraints. *IEEE Int. Conf. on Cont. Appl.*, pages 825–830, 2012.

[9] A. N. Bishop, T. H. Summers, and B. D. O. Anderson. Stabilization of stiff formations with a mix of direction and distance constraints. In *IEEE Int. Conf. on Cont. Appl.*, pages 1194–1199, 2013.

[10] U. Borrmann, L. Wang, A. D. Ames, and M. Egerstedt. Control barrier certificates for safe swarm behavior. *Analysis and Design of Hybrid Systems*, 48(27):68 – 73, 2015.

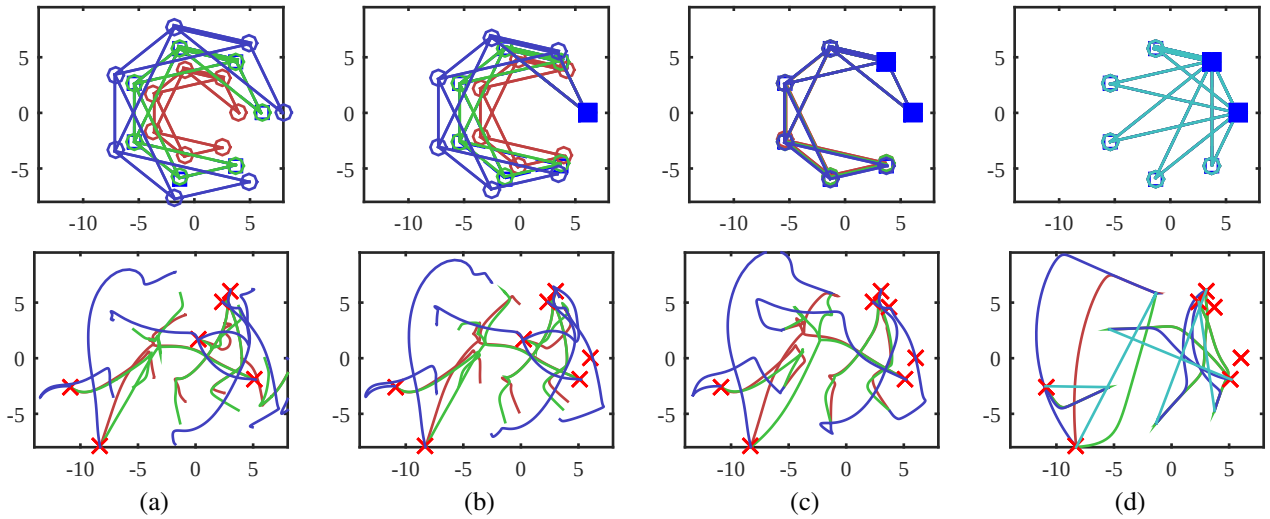

Fig. 3: Simulation results for the four scenarios with different number of leaders and topologies (see text). Top: final configurations; squares indicate leader agents. Middle: initial positions and trajectories. Colors: — Our controller; — Our controller with one distance measurements (between nodes 3 and 4); — Controller from [38]; — Controller from [14].

[11] A. K. Das, R. Fierro, V. Kumar, J. S. J. P. Ostrowski, and C. J. Taylor. A Vision-Based Formation Control Framework. In *IEEE Trans. Robot. Automat.*, volume 5, pages 813–825, 2002.

[12] J. P. Desai, J. Ostrowski, and V. Kumar. Controlling formations of multiple mobile robots. In *IEEE Int. Conf. on Robot. Automat.*, volume 4, pages 2864–2869, 1998.

[13] T. Eren. Formation shape control based on bearing rigidity. *International Journal of Control*, 85(9):1361–1379, 2012.

[14] A. Franchi, C. Masone, V. Grabe, M. Ryll, H. H. Bülthoff, and P. R. Giordano. Modeling and Control of UAV Bearing Formations with Bilateral High-level Steering. *The International Journal of Robotics Research*, 31(12):1504–1525, 2012.

[15] S. R. Lindemann and S. M. LaValle. Simple and efficient algorithms for computing smooth, collision-free feedback laws over given cell decompositions. *The International Journal of Robotics Research*, 28(5):600–621, 2009.

[16] Q. Lindsey, D. Mellinger, and V. Kumar. Construction of Cubic Structures with Quadrotor Teams. In *Robotics: Science and Systems*, 2011.

[17] G. L. Mariottini, F. Morbidi, and D. Prattichizzo. Vision-based localization and control of leader-follower formations. In *IEEE Int. Conf. on Robot. Automat.*, pages 2403–2408, 2007.

[18] S. Mastellone, D. M. Stipanović, C. R. Graunke, K. A. Intlekofer, and M. W. Spong. Formation control and collision avoidance for multi-agent non-holonomic systems: Theory and experiments. *The International Journal of Robotics Research*, 27(1):107–126, 2008.

[19] N. Michael, J. Fink, and V. Kumar. Cooperative manipulation and transportation with aerial robots. *Autonomous Robots*, 30(1):73–86, 2011.

[20] D. Morgan, S.-J. Chung, and F. Y. Hadaegh. Model predictive control of swarms of spacecraft using sequential convex programming. *Journal of Guidance, Control, and Dynamics*, 37(6):1725–1740, 2014.

[21] N. Moshtagh, N. Michael, A. Jadbabaie, and K. Daniilidis. Vision-Based, Distributed Control Laws for Motion Coordination of Nonholonomic Robots. *IEEE Trans. Robot. Automat.*, 25(4):851–860, 2009.

[22] R. Olfati-Saber and R. M. Murray. Distributed cooperative control of multiple vehicle formations using structural potential functions. In *IFAC World Congress*, pages 346–352, 2002.

[23] D. Panagou. Motion planning and collision avoidance using navigation vector fields. In *IEEE Int. Conf. on Robot. Automat.*, pages 2513–2518, 2014.

[24] D. Panagou, D. M. Stipanovič, and P. G. Voulgaris. Multi-objective control for multi-agent systems using lyapunov-like barrier functions. In *IEEE Int. Conf. on Decision and Control*, pages 1478–1483, 2013.

[25] A. Petitti, A. Franchi, D. D. Paola, and A. Rizzo. Decentralized motion control for cooperative manipulation with a team of networked mobile manipulators. In *IEEE Int. Conf. on Robot. Automat.*, 2016.

[26] G. Piovan, I. Shames, B. Fidan, F. Bullo, and B. Anderson. On frame and orientation localization for relative sensing networks. *Automatica*, 49(1):206–213, 2013.

[27] B. Servatius and W. Whiteley. Constraining plane configurations in computer-aided design: Combinatorics of directions and lengths. *SIAM Journal on Discrete Mathematics*, 12(1):136–153, 1999.

[28] J. Spletzer, A. K. Das, R. Fierro, C. J. Taylor, V. Kumar, and J. P. Ostrowski. Cooperative localization and control for multi-robot manipulation. In *IEEE Int. Conf. on Intel. Robots and Syst.*, pages 631–636, 2001.

[29] K. Sreenath and V. Kumar. Dynamics, Control and Planning for Cooperative Manipulation of Payloads Suspended by Cables from Multiple Quadrotor Robots. In *Robotics: Science and Systems*, 2013.

[30] G. Stacey and R. Mahony. A port-Hamiltonian approach to formation control using bearing measurements and range observers. In *IEEE Int. Conf. on Decision and Control*, 2013.

[31] C. Tomlin, G. J. Pappas, and S. Sastry. Conflict resolution for air traffic management: A study in multiagent hybrid systems. In *IEEE Trans. Automat. Contr.*, 1998.

[32] R. Tron and K. Daniilidis. An optimization approach to bearing-only visual homing with applications to a 2-D unicycle model. In *IEEE Int. Conf. on Robot. Automat.*, 2014.

[33] R. Tron, J. Thomas, G. Loianno, J. Polin, V. Kumar, and K. Daniilidis. Vision-based formation control of aerial vehicles. In *Workshop on Distributed Control and Estimation for Robotic Vehicle Networks*, 2014.

[34] R. Tron and R. Vidal. Distributed 3-D localization of camera sensor networks from 2-D image measurements. *IEEE Trans. Automat. Contr.*, 2014.

[35] Z. Wang and M. Schwager. Kinematic multi-robot manipulation with no communication using force feedback. In *IEEE Int. Conf. on Robot. Automat.*, 2016.

[36] D. Zelazo, A. Franchi, F. Allgöver, H. H. Bülthoff, and P. R. Giordano. Rigidity Maintenance Control for Multi-Robot Systems. In *Robotics: Science and Systems*, 2012.

[37] S. Zhao, F. Lin, K. Peng, B. M. Chen, and T. H. Lee. Distributed control of angle-constrained cyclic formations using bearing-only measurements. *Systems and Control Letters*, 63:12–24, 2014.

[38] S. Zhao and D. Zelazo. Bearing rigidity and almost global bearing-only formation stabilization. *IEEE Trans. Automat. Contr.*, PP(99):1–1, 2015.